Interpreting INEEL Vadose Zone Water Movement on the Basis of Large-Scale Field Tests and Long-Term Vadose Zone Monitoring Results

Earl D. Mattson,* Swen O. Magnuson, and Shannon L. Ansley

ABSTRACT

A review of the results from two large-scale field tests and vadose zone monitoring data at two facilities at the Idaho National Engineering and Environmental Laboratory (INEEL) has provided information to support development of a conceptual model of water movement in the highly heterogeneous vadose zone beneath two INEEL facilities. Both of the large-scale field tests were ponded water infiltration tests that approached the size of the two facilities. An assembly of perched water wells, neutron access tubes, and tensiometers have been used to monitor water movement beneath these sites. Once water has percolated through the surficial sediment at these facilities, the presence of the surficial sediment–basalt interface results in some perching of the percolated water with limited lateral movement. Water movement in basalt formations is mainly gravity-dominated in preferential fracture pathways and rubble zones and results in rapid vertical flow especially frequently under conditions of positive hydrostatic head. Detection of wetting front advance is typically not sequential with depth and has been shown to vary between episodic infiltration events. At the basalt–sediment interface of the interbeds, perched water is often detected and has resulted in more lateral spreading of recharge than at the surficial sediment–basalt interface. Gaps in the sedimentary interbeds will allow some of the recharge water to bypass the interbeds and rapidly continue toward the aquifer. This complex water movement in the vadose zone beneath the INEEL supports the need to control surface infiltration, identify gaps and the lateral continuity of the interbeds, and investigate the influence of nearby surface water sources on perched water movement beneath these two facilities.

Water movement through the vadose zone beneath waste disposal facilities at the INEEL has been extremely difficult to quantify because of the spatial distribution of infiltration into a complex heterogeneous geologic vadose zone. Seasonal changes in precipitation and snowmelt events result in temporal variations in infiltration at the soil surface. Surface water runoff and surface infiltration are complicated by anthropogenic disturbances in the surficial soil, such as removal of vegetation and channeling by natural and artificial surface contours and water diversion features. As water infiltrates through the vadose zone, it initially encounters relatively thin surficial sediments overlying a complex stratigraphic package of fractured and interbedded basalt flows. This geologic framework, characteristic of the Eastern Snake River Plain, exhibits high spatial variability in physical, hydrologic, and geochemical properties. To date, most descriptions of these properties are based on vertical borehole information that is inherently limited because of its point-source nature. Downhole instrumentation and long-term monitoring data have provided some small-scale properties measurements. Large-scale measurements are more difficult to obtain as well as logistically cumbersome, costly, and often difficult to interpret.

Of the facilities on the INEEL currently being investigated to assess their potential environmental impacts, two have significant potential vadose zone contamination sources. These are the Subsurface Disposal Area (SDA) at the Radioactive Waste Management Complex (RWMC) and the Idaho Nuclear Technology and Engineering Center (INTEC). Both facilities have undergone extensive vadose zone characterization efforts and have monitoring instrumentation systems in the vadose zone.

The characterization and monitoring activities have been conducted with the goal of understanding the mechanisms controlling water and contaminant movement in the lithologically complex subsurface at the sites. This conceptual understanding is embedded in simulation models that assist in the selection between possible remedial actions and in improving long-term monitoring systems in the vadose zone. The conceptual model of water and contaminant movement is developed from information gained from the facility characterization and monitoring programs, and from infiltration experiments conducted on the INEEL to improve understanding of water movement in the subsurface. These experiments were conducted at scales approaching those beneath the facilities of interest on the INEEL.

Experiments at the facility-scale allow examination of percolation processes at a scale adequate to include interaction between temporal infiltration processes and the complex underlying geologic structure. Disadvantages to experiments at the facility-scale include difficulties in experimental control and decreased data density.

This paper presents an overview of the large-scale experiments that have been conducted at the INEEL and describes what has been learned from the experiments and from characterization and monitoring activities at the INEEL. This information is summarized in a description of mechanisms controlling water movement as it transits the geologically complex vadose zone.

BACKGROUND

The INEEL, originally established in 1949 as the National Reactor Testing Station, is a USDOE-managed

E.D. Mattson, S.O. Magnuson, and S.L. Ansley, Idaho National Engineering and Environmental Laboratory, Idaho Falls, ID 83415-2107. Received 28 Mar. 2003. Special Section: Understanding Subsurface Flow and Transport Processes at the Idaho National Engineering & Environmental Laboratory (INEEL) Site. *Corresponding author (matted@inel.gov).

Published in Vadose Zone Journal 3:35–46 (2004).

677 S. Segoe Rd., Madison, WI 53711 USA

Abbreviations: CERCLA, Comprehensive Environmental Response, Compensation, and Liability Act; CFA, Central Facility Area; INEEL, Idaho National Engineering and Environmental Laboratory; INTEC, Idaho Nuclear Technology and Engineering Center; LSIT, Large Scale Infiltration Test; RWMC, Radioactive Waste Management Complex; SDA, Subsurface Disposal Area.

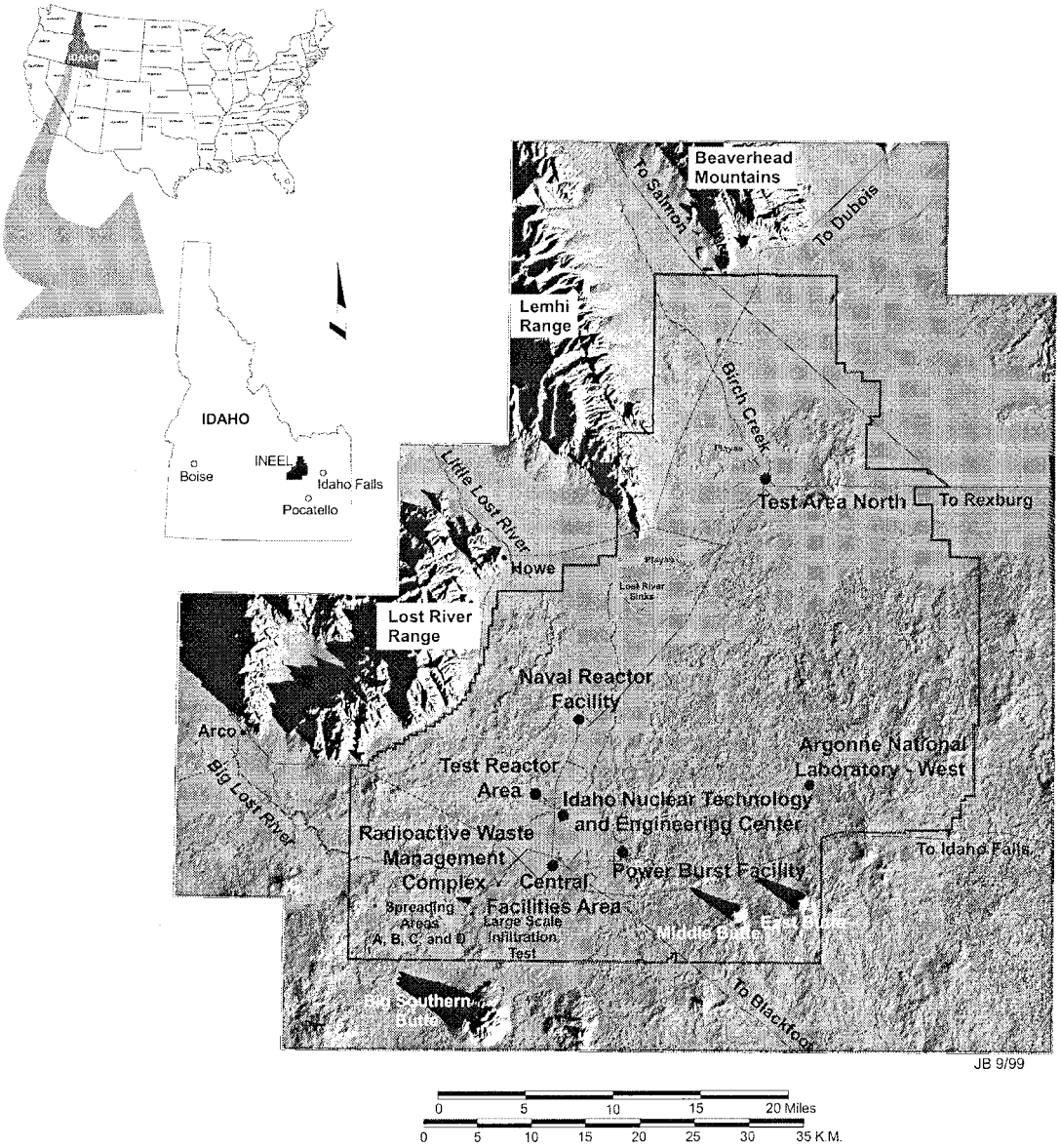

Fig. 1. Site map of the Idaho National Engineering and Environmental Laboratory.

reservation historically devoted to energy research and related activities. Located in southeastern Idaho (see Fig. 1), the site occupies 2305 km^2 in the northeastern region of the Snake River Plain. Primary technical and industrial facilities are indicated on Fig. 1. The surrounding land surface is a relatively flat, semiarid, sagebrush desert. Predominant relief is manifested either as volcanic buttes jutting up from the desert floor or as unevenly surfaced basalt flows or flow vents and fissures. Elevations on the INEEL range from 1460 m in the south to 1802 m in the northeast, with an average elevation of 1524 m above sea level (Irving, 1993). Mountain ranges border the INEEL on the north and west.

Idaho National Engineering and Environmental Laboratory surface water features include the Little Lost River, Big Lost River, and Birch Creek (Fig. 1). Normally, water is diverted for irrigation or hydropower before reaching the INEEL and only flows onto the site when the snow pack provides spring runoff in excess of the irrigation requirements. The Big Lost River enters the INEEL from the west and terminates at the Lost River Sinks north of the Naval Reactor Facility. Flow from the Big Lost River can also be diverted to spreading areas west and southwest of the RWMC. Birch Creek and the Little Lost River enter the site from the northwest and also terminate within the site boundary. Beneath the INEEL, the regional groundwater system, the Snake River Plain Aquifer, generally flows from the northeast toward the southwest.

The SDA is located in the southwest portion of the INEEL. Low-level, mixed, and transuranic radioactive waste was buried in shallow pits and trenches in the SDA from 1952 until 1970. Since 1970, transuranic waste has been stored in aboveground facilities. Mixed-waste disposal ceased in 1982; however, low-level waste is currently being buried in a portion of the SDA. The SDA overlies a thick stratigraphic sequence composed

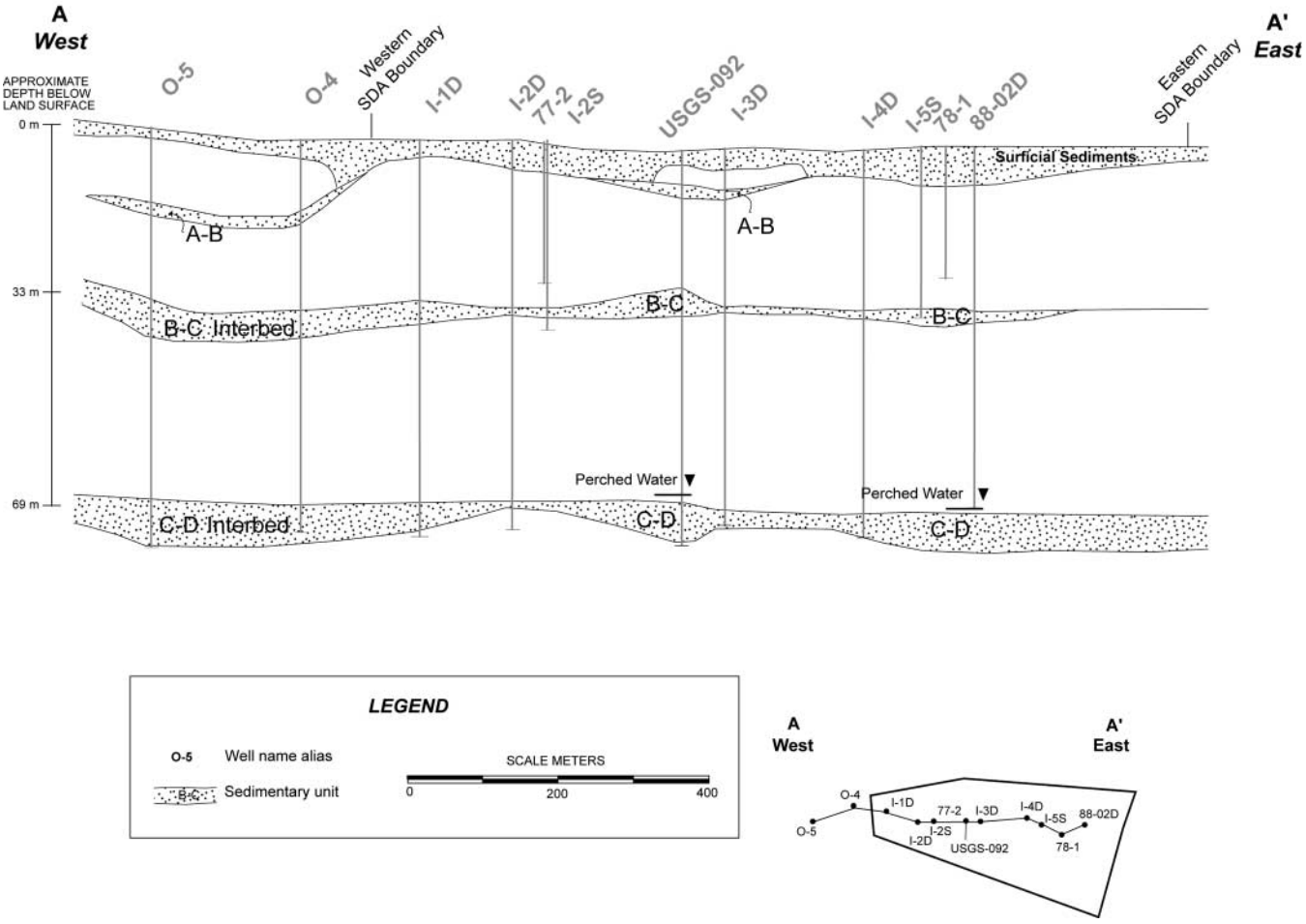

Fig. 2. Stratigraphic illustration of the sedimentary interbed structure beneath the Subsurface Disposal Area.

primarily of fractured basalts that are occasionally interrupted by fairly extensive sedimentary interbeds that were deposited during extended periods of volcanic quiescence (Fig. 2). The three upper most interbeds beneath the SDA, named the A–B, B–C, and C–D interbeds, are generally located at approximately 10, 33, and 69 m below land surface. Each of the interbeds is known to have some discontinuities. The A–B interbed is fairly discontinuous and generally only exists beneath the northern half of the SDA, whereas the C–D interbed is the most continuous beneath the facility.

There is a variety of vadose zone monitoring equipment installed in boreholes at the SDA. Shallow instrumentation, installed within the surficial sediments, consists of 27 neutron access tubes, 78 commercial-grade soil moisture capacitance sensors, and 41 solution samplers (lysimeters). Deeper instrumentation is primarily located within or immediately above interbeds and consists of 30 advanced tensiometers installed at depths up to 74 m, 29 solution samplers, and up to eight wells that have shown perched water at time times. A detailed summary of the SDA's history, local geology, waste description, monitoring network, and extent of contamination in the vadose zone can be found in an INEEL report by Holdren et al. (2002).

Idaho Nuclear Technology and Engineering Center, formerly the Idaho Chemical Processing Plant, is a multipurpose facility located approximately 12 km (7.5 mi) northeast of the SDA. Constructed in 1951, INTEC initially received and stored spent nuclear fuels, processed the fuels to recover ^{235}U, and handled all waste generated by those functions. After 1992, INTEC began receiving and temporarily storing spent nuclear fuel and waste fission products resulting from spent fuel recovery processes. High-level liquid waste generated from these operations was stored in eleven 1100-m^3 and four 110-m^3 underground storage tanks. The area containing these tanks is called the tank farm. Contaminants found in the soils of the tank farm are the result of accidental releases and leaks from process piping, valve boxes, and sumps associated with tank operations and are also the result of cross-contamination from general operations and maintenance excavations. There is no evidence that the tanks themselves have leaked. Additional vadose zone contamination resulted from disposal of service wastewater into the percolation ponds located immediately south of the INTEC facility.

The vadose zone monitoring system at INTEC (consisting of tensiometers, lysimeters, piezometers, soil moisture probes, and temperature sensors) is designed to monitor three distinct intervals: the surficial alluvium between 0 and 18 m below land surface, the shallow perched

zone between 18 and 60 m, and the deep perched zone between 60 m and the surface of the aquifer at approximately 140 m. The thickness of surficial sediments at INTEC ranges from 8 to >15 m and generally contains more than 50% gravel-size material. Commonly, there is a layer of silt- or clay-size material at the interface of the surficial alluvium and the uppermost basalt. The deeper geologic structure beneath the INTEC facility is similar to that observed at the SDA but exhibits less extensive lateral basalt flow and interbed continuity (Forsythe, 2003). Compared with the SDA, the INTEC monitoring system is not as extensive and does not have a long monitoring history. The most lengthy and continuous perched water information (1992–2000) was recorded by pressure transducer–data logger pairs installed in several perched water wells in the northern half of INTEC. Approximately 76 vadose zone monitoring wells exist at the INTEC facility; most of these wells monitor the shallow and deep-perched water zones. Tensiometers were installed in approximately 30 locations to observe soil matric potentials.

Numerous field investigations pertaining to infiltration of water have been conducted at the INEEL. Two of these field investigations, the Large Scale Infiltration Test (LSIT) and the Spreading Area Tracer Test, approach the scale of the facilities. In both of these field investigations, water was supplied to the soil surface under sustained positive hydrostatic head and the resulting movement of water in the subsurface was monitored to assess the influence of heterogeneity within the fractured basalt and the sedimentary interbeds. A short overview of each experiment follows.

LARGE-SCALE INFILTRATION TEST

The LSIT was conducted in 1994 and was part of a coupled large-scale aquifer pump test and an infiltration test located approximately 1.5 km south of the SDA (Fig. 3). The infiltration basin was a 180-m (600-foot) circular impoundment approximately 1.4 m deep. During a period of 36 d water from the aquifer pumping test was discharged into the impoundment at approximately 2725 m^3 d^{-1}. Much of the soil was removed from the basin to build the earthen berm partially exposing the surface of the basalt. The basalt surface was highly uneven, with approximately 80% covered by a thin layer of silty soil while the remaining 20% was exposed elevated basalt. The average infiltration rate was about 0.11 m d^{-1} (Dunnivant et al., 1998). After approximately 6 d of adding water to the basin, conservative and reactive tracers were added in an 11-d finite pulse. Subsurface migration of infiltrating water and tracers was monitored by several techniques using monitoring wells and surficial geophysics.

The 70 monitoring wells were aligned on spokes emanating from the center of the basin. Wells were located at four selected intervals, or rings, spaced from the center of the basin. The innermost ring was within the basin, and subsequent rings were approximately 15-, 90-, and 230-m (50, 300, and 750 ft) from the edge of the basin, respectively. The primary zone of interest was from the land surface to the first continuous interbed; therefore, the monitoring wells ranged from a depth of 15 to 55 m. The wells were completed with PVC casing or carbon steel casing. Monitoring included neutron probe measurements, direct current resistivity, and water sample collection through the monitoring wells and lysimeters.

SPREADING AREA TRACER TEST

The Big Lost River diversion dam was built in 1958 to control spring flooding and is approximately 4 km northwest of the SDA. During years of large snowpack in the mountains, the Big Lost River flows onto the INEEL and a portion of the water is diverted into four impoundments called Spreading Areas A through D (See Fig. 3). The total storage capacity of these impoundments is 4.7×10^7 m^3 (38 000 acre-ft). No flow was diverted into the spreading areas until 1965 because of the low flow in the Big Lost River. Figure 3 illustrates the discharge boundaries of the spreading areas. Records indicate that there have been three major periods, or diversion sets, where the spreading areas received water from the Big Lost River. In the first set, from 1965 to approximately 1977, water was diverted into the spreading area on a yearly basis. The second diversion period, from 1982 to 1986, was shorter in duration than the first but had higher flow rates. The last diversion set occurred from 1994 to 1999, and the volume of diverted water was low relative to the first two diversion sets. No water has been diverted into the spreading areas since 1999.

In 1999, the USGS conducted a tracer test by adding a conservative tracer (naphthalene sulfonate) to the water in the two spreading areas closest to the SDA. A summary of this tracer test and an interpretation of its results can be found in Nimmo et al. (2002, 2004). Perched water monitoring wells at the sedimentary interbeds and groundwater wells were periodically sampled for the detection of the tracer.

WATER SOURCES: NATURAL AND ANTHROPOGENIC

At the INEEL, the majority of contaminants of concern are inorganic and are transported through the vadose zone as dissolved species in water. The spatial and temporal distribution of infiltration at the RWMC and INTEC appears to be the major parameter that controls the flux of contaminants from the source zone. Water sources include diffuse precipitation in the form of rain and snow, rivers entering a closed basin, and water disposal at the land surface.

Precipitation is a highly variable source of water at the INEEL. Based on a 38-yr historical record analyzed by Clawson et al. (1989), the annual average precipitation was approximately 22 cm yr^{-1} (6.0×10^{-4} m d^{-1}) with a maximum of 36 cm yr^{-1} (9.9×10^{-4} m d^{-1}) and a minimum of 11 cm yr^{-1} (3.0×10^{-4} m d^{-1}). Heaviest precipitation usually occurs in the spring and early summer and most of the precipitation events are <0.25 cm d^{-1} (2.5×10^{-3} m d^{-1}). However, thundershowers can

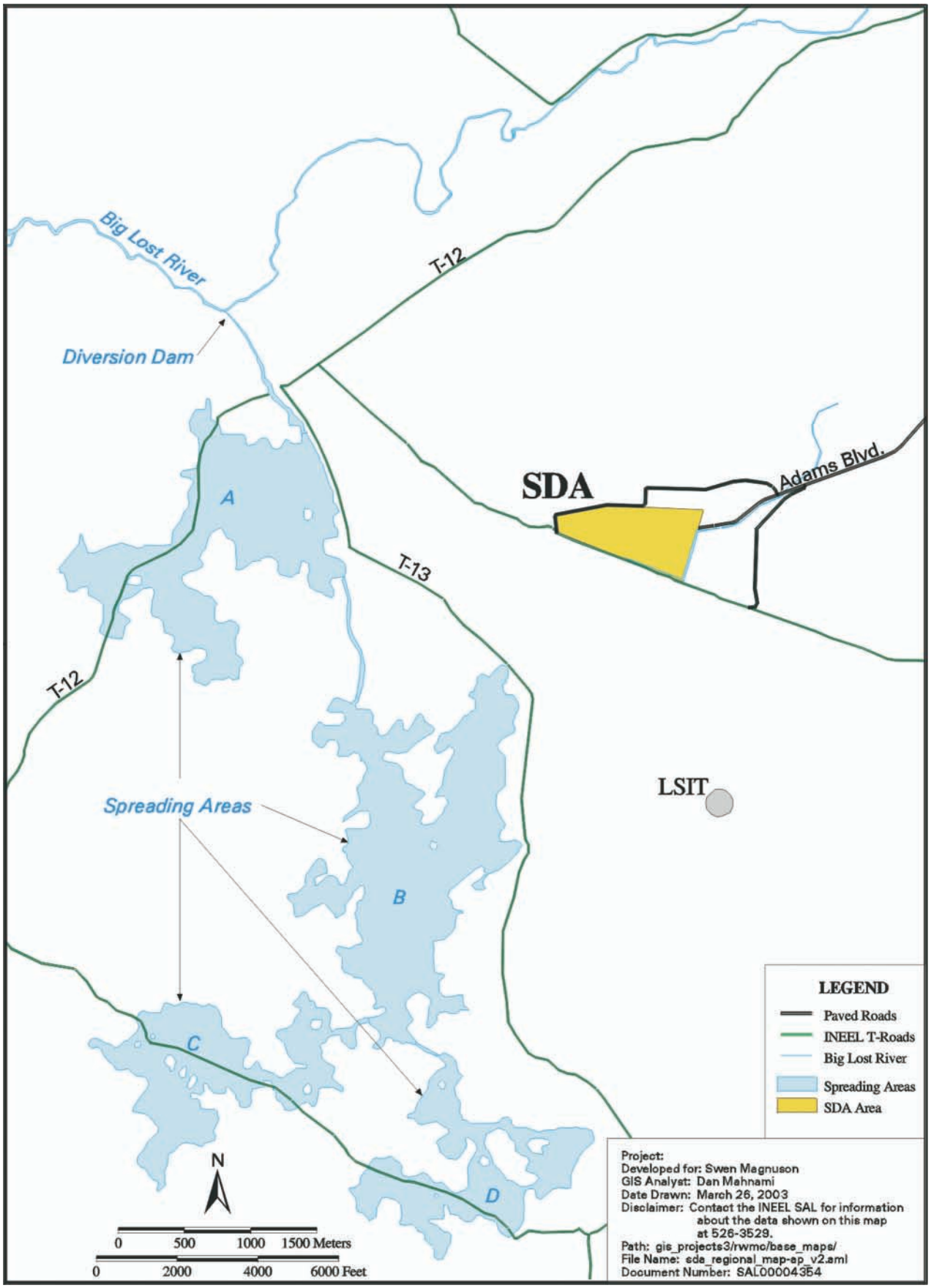

Fig. 3. Location of the Big Lost River, the spreading areas and the large-scale infiltration test in relationship to the Subsurface Disposal Area.

produce a significant amount of precipitation in a short time. The historic record of precipitation from the Central Facility Area (CFA) weather station, approximately 8 km northeast of the SDA, and 5 km south of INTEC, indicates precipitation intensities >2.5 cm h^{-1} (6.0×10^{-1} m d^{-1}) in eight of the 38 yr at CFA. The long CFA precipitation record is likely representative of conditions at the southern portion of the INEEL (Magnuson, 1993), including both the SDA and INTEC.

A typical winter produces snow cover from mid November to mid April (Clawson et al., 1989). The CFA snowfall records indicate an average snowfall of 0.7 m and ranges from 0.17 to 1.5 m. Moderate to strong surface winds cross the plains at the INEEL and redistribute much of the snow, resulting in drifts exceeding 1 m in depth.

SUBSURFACE DISPOSAL AREA–SPECIFIC WATER SOURCES

Rivers, impoundments, and water discharges are not major recharge sources at the SDA. The Big Lost River is located approximately 3 km north of the SDA (Fig. 3). Although the Big Lost River is 9 to 12 m higher than the SDA, the river is topographically isolated from the SDA and a study examining the potential effects of the upstream Mackay Dam failure concluded that the resulting flood would not inundate the SDA (Koslow and Van Haaften, 1986). Anthropogenic discharge of water is small and has no effect on surface infiltration (Holdren et al., 2002). However, recharge from the Big Lost River diversion into the spreading areas has been confirmed to be a source of perched water associated with the C–D interbed (Nimmo et al., 2002) beneath the SDA (Fig. 2).

Intense summer thunderstorms and melting snow create surface water ponds, which are the major recharge source at the SDA. The SDA land surface has been severely altered by the creation of excavated pits and trenches for waste disposal. These excavation activities destroyed many of the native plant communities and recontoured surface topography as a result of mounding soil on top of waste pits, building roads, covering trenches, and constructing soil vaults. As a result, local surface ponding after heavy summer thunderstorms or early spring snowmelt is common. During the winter months, melt-water runoff atop frozen soil creates localized surface ponds and has enhanced recharge (Martian and Magnuson, 1994; Bishop, 1996). Much of this surface water infiltrates into the ground, although a portion is diverted off-site through a series of unlined ditches. It is likely that these episodic high-intensity precipitation events and melting snow contribute to the bulk of recharge through the SDA.

Estimates of infiltration rates in undisturbed natural sediments adjacent to the SDA are small and suggest that approximately 5% of the annual precipitation infiltrates past the root zone. Cecil and others (1992) measured the infiltration rate using three separate methods in undisturbed soil immediately north of the SDA. Chlorine-36 and T profiles were determined to approximately 5.5 m in depth. These measurements indicated infiltration rates of 0.71 and 1.1 cm yr^{-1} (1.9×10^{-5} and 3.0×10^{-5} m d^{-1}). An infiltration rate using the tritium mass balance method gave a rate of 0.89 cm yr^{-1} (2.4×10^{-5} m d^{-1}). The Darcian flux beneath the root zone (below 3.7 m in this case) for a 4-yr period averaged 0.36 cm yr^{-1} (9.9×10^{-6} m d^{-1}). These low infiltration rates are considered to represent the background infiltration rate and are often used in the SDA Comprehensive Environmental Response, Compensation, and Liability Act (CERCLA) performance assessment numerical transport models as 1 cm yr^{-1} (2.7×10^{-5} m d^{-1}) (Magnuson and Sondrup, 1998).

Infiltration estimates for CERCLA modeling activities through the SDA suggest that the infiltration rate may be almost an order of magnitude greater inside the SDA compared with diffuse recharge outside the SDA (Martian, 1995). At the SDA, McElroy (1990, 1993) and Bishop (1996) measured a wide variety of infiltration rates using neutron moisture measurements from the neutron access tubes. This monitoring network was enhanced in the early 1990s to a total of 27 measuring locations located throughout the SDA. Net infiltration was calculated from changes in the measured moisture content profile below a depth of approximate 1 m (3 ft), assuming changes from land surface to 1 m were due to evapotranspiration. During 5 yr, (1989, 1993–1996) sufficient data were available to estimate the net infiltration. These estimates ranged from 0.3 to 55.9 cm yr^{-1} (8.2×10^{-6} to 1.5×10^{-3} m d^{-1}) depending on the year and location of measurement. They attributed these highly variable estimates to snow drifting and plowing, presence or absence of frozen soil, soil disturbance, topographic variations, and local drainage patterns.

On the basis of the variable infiltration suggested by McElroy (1990, 1993) and Bishop (1996), Martian (1995) developed an infiltration distribution map for the SDA to be used in the risk assessment models. Martian simplified the infiltration to the SDA by suggesting that it could be adequately described by using three constant infiltration rates of 0.64, 3.68, and 24.1 cm yr^{-1} (1.8, 10, and 66×10^{-5} m d^{-1}). The location of these zones was based on topographic considerations and inverse modeling to the neutron monitoring moisture profiles. The spatial average of Martian's infiltration rates assigned inside the SDA is 8.5 cm yr^{-1} (2.3×10^{-4} m d^{-1}), a value much higher than that considered to be background ($\approx$1 cm yr^{-1} [$\approx 2.7 \times 10^{-5}$ m d^{-1}]). The higher infiltration rate through the SDA surficial soils are supported by greater soil water potential measurements beneath the SDA as compared with those outside the SDA (McElroy and Hubbell, 2003).

Although the potential of the Big Lost River flooding the SDA is low, late winter rain and snowmelt events have produced three occurrences (1962, 1969, 1982) of focused recharge at the SDA. Vigil (1988) estimated the amount of water that infiltrated through the SDA for each event using historical documentation that described the size and location of the pits and trenches were active at the time of the flood event. Vigil concludes that 34 000 m^3 infiltrated during 1962, 43 000 m^3 of water for infiltration in 1969, and approximately 10 000 m^3 of water during the last flooding event in 1982.

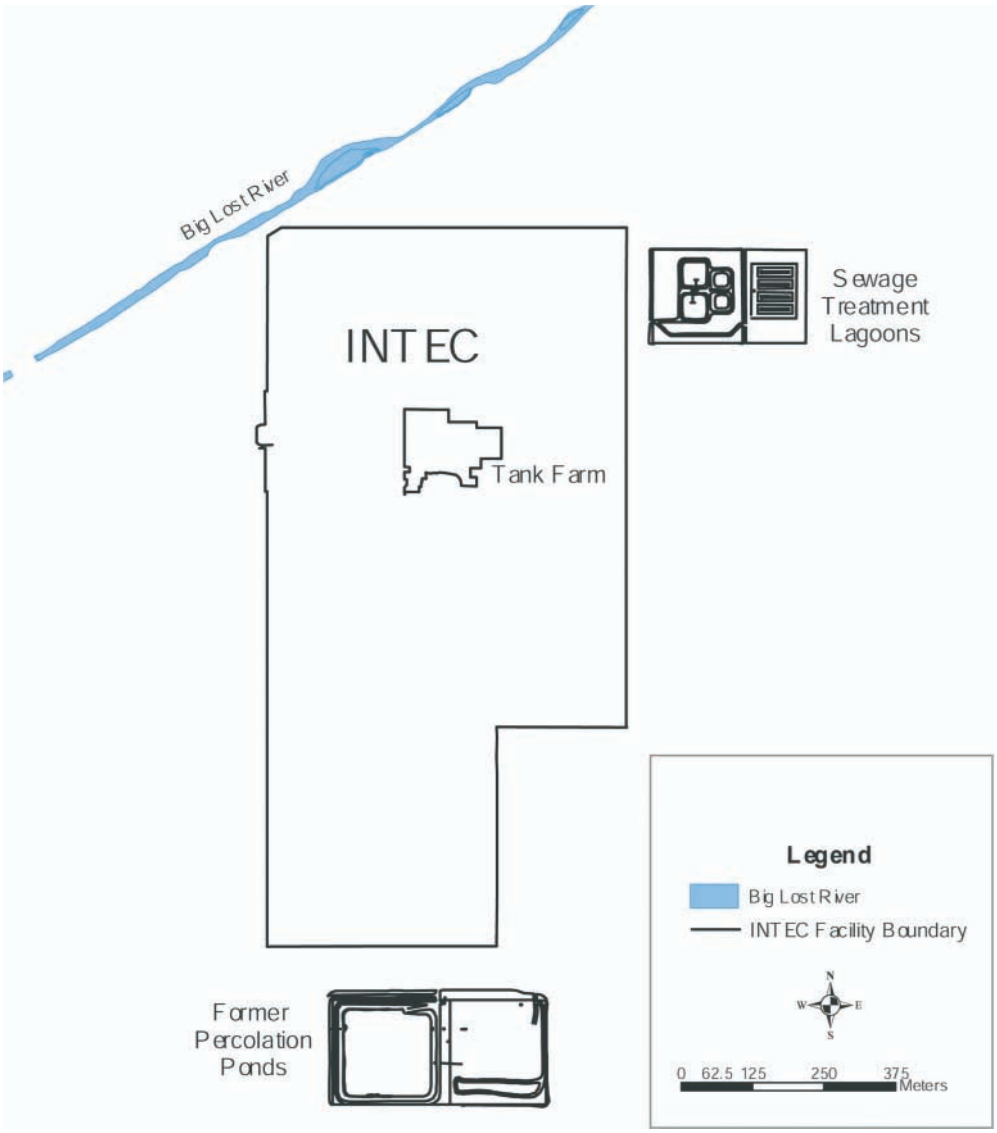

Fig. 4. Site map of Idaho Nuclear Technology and Engineering Center illustrating the location of the major recharge sources at the surface.

These singular infiltration events have been incorporated into numerical models (Magnuson and Sondrup, 1998), and these volumes are approximately equal to the annual recharge through the SDA.

IDAHO NUCLEAR TECHNOLOGY AND ENGINEERING CENTER–SPECIFIC WATER SOURCES

In contrast to the SDA, anthropogenic water sources at INTEC have been the major contributors to surface infiltration resulting in the formation of a significant and persistent perched water body in the northern part of the facility centered beneath the tank farm and another in the south, centered beneath the former service wastewater disposal ponds (Fig. 4). Anthropogenic recharge sources include wastewater disposal ponds, septic systems, nuclear fuel storage basins, steam condensate discharges, landscape irrigation, facility maintenance operations and firewater discharges, and leaking underground pipelines. Natural recharge sources at INTEC are the Big Lost River, located <60 m northwest of the facility boundary, and precipitation. Flow in the river channel within the INEEL boundaries is historically intermittent and dependent upon upstream irrigation and hydropower demands in the Big Lost River basin area and on diversion practices at the SDA spreading areas. The last recorded flow in the channel adjacent to INTEC was May 2000. Before then, recorded flow in the channel occurred from 1995 through 1999, in 1993, and during the years before 1987. By volume, the largest of the recharge sources are the Big Lost River and the former service wastewater disposal ponds located south of the main facility. Idaho Nuclear Technology and Engineering Center service wastewater is currently discharged in new percolation ponds located approximately 3 km (2 miles) southwest of the old ponds, thereby eliminating the largest anthropogenic recharge source in the area.

WATER MOVEMENT AT THE SURFICIAL SEDIMENT–BASALT INTERFACE

As water infiltrates through surficial sediments at the INEEL, it eventually encounters a basalt flow interface.

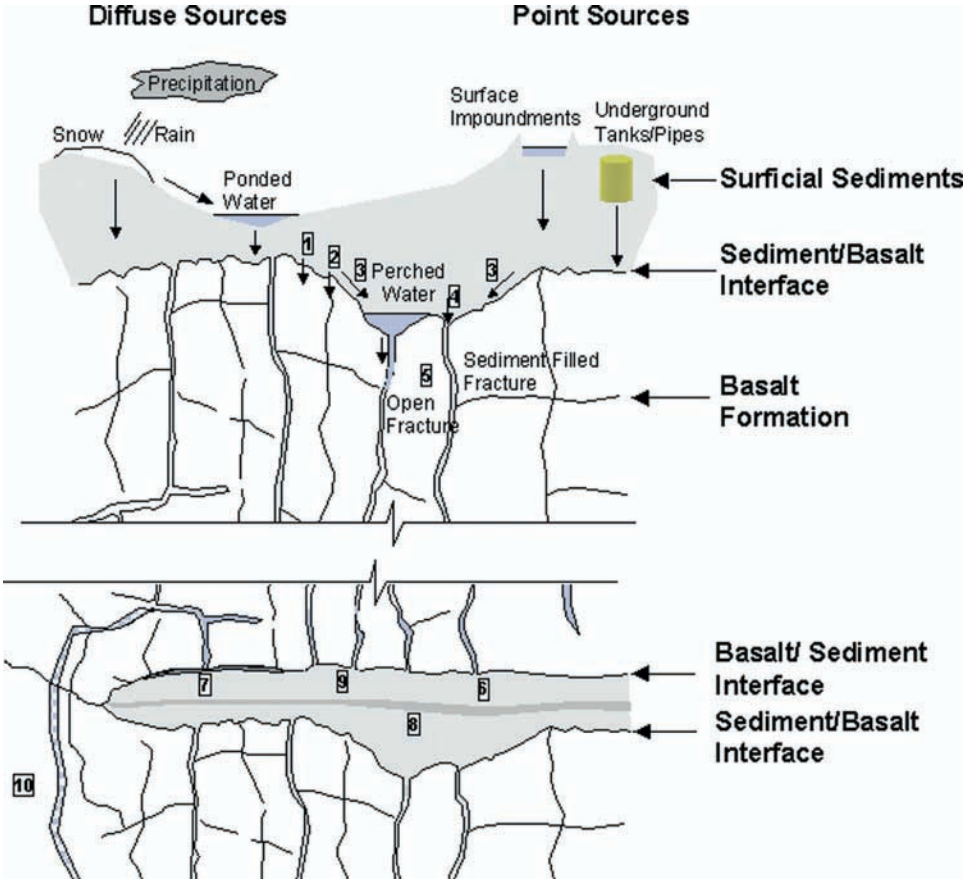

Fig. 5. Mechanism controlling water recharge at the upper sedimentary–basalt interface and at subsurface sedimentary interbeds.

Multiple mechanisms are possible by which water can continue moving downward through this interface and are illustrated graphically in Fig. 5. The first mechanism illustrated in Fig. 5 is movement from the pore space of the sediments into the pore space of the basalt matrix. A second mechanism, closely related to the first, consists of water movement from the pore space in the sediments into a very small aperture fracture. In a third mechanism, if a sufficient flux of moisture moves across the sediments, perched water can occur along with lateral movement along the interface. A fourth possible mechanism of water movement across this interface is when water moving laterally or vertically encounters a sediment-filled fracture into the underlying basalt. The fifth, and potentially dominant, mechanism by which water crosses the sediment–basalt interface occurs when perched water accumulates at the interface and encounters a high permeability network of open fractures.

Data collected from large field tests and vadose zone monitoring instrumentation at the INEEL indicate that the upper sediment–basalt interface is typically not a long-term barrier to percolation of surface water. Temporary perching of water has been documented at the uppermost sediment–basalt interface beneath the SDA (Hubbell et al., 2002), indicating that episodic snowmelt rates within the SDA are of sufficient magnitude to exceed the infiltration capacity of the upper basalt surface.

Some lateral movement along the basalt surface should be expected when the moisture flux moving vertically through the surficial sediments is greater than the hydraulic conductivity of the underlying basalt matrix, or when there is a basal clay facies at the sediment–basalt interface. Lateral movement of water along the sediment–basalt interface has been documented within the SDA (McElroy, 1993). In a study described by Hull and Bishop (2004), analysis of the Cl^-/Br^- ratios in surficial sediments indicate $MgCl_2$ brines used for dust suppression on roads within the SDA primarily spread 13 m from the treated roads. These monitoring results suggest that lateral movement of water and dissolved solutes at the uppermost sedimentary–basalt interface does occur, but it is not extensive.

At INTEC, despite the large recharge flux from the Big Lost River, the former percolation ponds, and the sewage treatment pond, lateral spreading at the surficial sediment–basalt interface is minimal. Beneath the former percolation ponds, perched water boundaries in the surficial alluvium rarely extend much beyond the pond perimeters (Cecil et al., 1991). The mechanism for this lack of lateral spread may be due to the much coarser surficial sediments present at INTEC allowing the water to find pathways into the basalt, the lack of a basal clay often found at the interface, or a highly fractured basalt formation at the interface.

WATER MOVEMENT WITHIN BASALT FORMATIONS

The movement of water within fractured basalt is difficult to quantify because of the extreme spatial heter-

ogeneity of the individual basalt flow and the interrelationship between basalt flows. The Eastern Snake River aquifer and vadose zone are composed of numerous basalt lava fields. Each basalt flow, on average, is approximately 7 m (23 ft) thick (Knutson et al., 1992). Each flow generally has an underlying rubble zone and develops a characteristic fracture pattern as a result of cooling. The result is a complex network of fractures and rubble zones that provide pathways for the movement of water in the vadose zone. Smith (2004) describes the regional geologic setting, origin, and evolution of the Snake River Plain aquifer and vadose zone.

When the water is supplied to the soil surface under positive hydrostatic head (e.g., LSIT, the spreading areas, INTEC, and the flooded SDA pits), the primary water movement in the basalt flows will be within the fracture network and rubble contact zones between basalt flows. The fractures and rubble zones will control the movement of water because of their high permeability compared with the competent basalt matrix. Water infiltration results in a rapid vertical advance of a wetting front through the basalt portion of the subsurface. Monitoring results from the LSIT (Dunnivant et al., 1998) indicated that beneath the infiltration pond, wetting front advance averaged about 5 m d^{-1}, although the range was highly variable (1.4–17.7 m d^{-1}). Water did not progress as a unified front sequentially wetting each zone as a function of depth beneath the pond. Vertical movement of the water through the fractured basalt vadose zone was observed; however, there was no evidence of lateral water movement to the monitoring locations 15 m (50 ft) outside the pond boundaries.

Unsaturated flow in fractures may have been recorded for the slow snowmelt wetting front advancement that was documented to a depth of 17.3 m beneath the SDA. Hubbell et al. (2002) used advanced tensiometers to monitor the wetting front advance at a variety of depths during the 1999 snowmelt. They calculated wetting front advances rates of about 0.1 m d^{-1} in the uppermost basalt formation. Although the advanced tensiometer data indicated short-term perched water at the surficial sediment–basalt interface (A–B), the deeper basalt matrix never became saturated during this infiltration event. This SDA snowmelt wetting front advance rate was approximately 10 to 100 times less than that estimated under near continuous ponding conditions at the LSIT.

Other long-term monitoring studies suggest that the flow mechanism and/or the flow pathways may be temporally variable. Advanced tensiometers at a field site in Idaho Falls (Hubbell et al., 2002) monitored the progression of the first arrival of a wetting front as a function of depth. Four separate infiltration events were identified between 1996 and 1999. The upper most tensiometer was located at the sediment–basalt (A–B) interface. Four additional tensiometers were placed in the fractured basalt to a depth of 15.5 m. The sequence of the wetting front advance in the fractured basalt, as determined from advanced tensiometer response, was typically not correlated with depth. Furthermore, the pattern of wetting front advance was not consistent between the four infiltration events. These results suggest that the flow pathways in the fractures are a function of the infiltration event and likely the magnitude and duration of the ponding of water at the sediment–basalt interface.

WATER MOVEMENT NEAR SEDIMENTARY INTERBEDS

Perched water is commonly found in the vadose zone beneath the SDA and INTEC and is associated with areas along the Big Lost River, spreading areas, and other areas that have a high volume of recharge at the INEEL. The exact physical mechanism causing perching in the INEEL vadose zone is unknown but is hypothesized to include the following (Cecil et al., 1991): (i) low permeability of interbeds compared to fractured basalt, (ii) low permeability at basalt interflow zones due to intense heating, (iii) reduced permeability due to dense less fractured basalt zones, and/or (iv) infilling of fractures in the basalt near the upper contact of a basalt interflow. Although analysis by Cecil et al. (1991, p. 31) suggests that basalt flow contacts were often responsible for perching in a well near the percolation ponds by INTEC, long-term monitoring and field test results suggest that sedimentary interbeds within the basalt formation have a larger effect on the creation of perched water and its lateral extent.

The physical mechanisms that could account for perching as described by Cecil et al. (1991) can be applied to the interbeds layers at INEEL. The first mechanism to cause perching at the interbeds is a permeability contrast. In this case, the interbed material would have a lower permeability than that of the overlying fractured basalt. Smith (2004) and Nimmo et al. (2004) discuss the geologic conceptual model and provide supporting data on permeability contrasts between the basalt formation and the interbed material. Applying the second mechanism, alteration of the sedimentary material due to the heating of the interbed surface material may create a low permeability zone along the upper surface of the interface sediments and create perched water conditions on top of the sedimentary interbed. Third, low permeability lenses within the interbeds may create a sufficient permeability contrast to create perched water within and above the interbed. Finally, infilling of fractures with fine-grained material at the basalt–sedimentary interbed could effectively seal the interface between the basalt and the sedimentary interbed. These perching mechanisms associated with the basalt–sedimentary interface are illustrated in Fig. 5 (Items 6–9).

Chemical detection at interbeds deeper in the vadose zone indicate that horizontal spreading of solutes increases as a function of depth. Chloride from the $MgCl_2$ brine applications to roads within the SDA was detected in a lysimeter sample at the B–C interbed 110 m north of the nearest treated road (Hull and Bishop, 2004). Horizontal lateral spreading of the Cl^- at the B–C interbed is approximately three times the maximum distance of that detected in the surficial sediments. Although the Cl^- detection could either support a conceptual model of lateral spreading along basalt interfaces with subsequent detection at the interbed or vertical trans-

port through the basalt formation with subsequent lateral movement along the basalt–sedimentary interface, data from the LSIT would suggest that the second conceptual model would be more plausible.

Mechanisms associated with the basalt–sedimentary interface results in a diversion of vertical flow of water in the basalt above interbed surfaces. During the LSIT, water moved vertically downwards in the basalt formation (Dunnivant et al., 1998), despite passing through four distinct basalt flows above the sedimentary interbed (Wood and Norrell, 1996). Lateral spreading of water in the vadose zone was only documented when it reached a sedimentary interbed at 55 m and flowed along topographic lows immediately above this interbed (Dunnivant et al., 1998). Rapid detected tracers in a monitoring well at the C–D interbed beneath the SDA that were placed in spreading areas more than a kilometer away are hypothesized to travel through saturated basalt fractures, tension cracks, lava tubes, or rubble zones rather than through the interbeds themselves Nimmo et al. (2002).

Defining the sources and lateral extent of perched water in the vadose zone has been a major focus of INTEC investigations. Three distinct perched water zones exist beneath INTEC: (i) at the surface alluvium–basalt interface, (ii) a shallow perched zone associated with interbeds at the 33- and 43-m (110- and 140-ft) depths, and (iii) a deep perched zone associated with an interbed at the 115-m (380-ft) depth (Forsythe, 2003). One former conceptual model assumed that the shallow perched water zone was laterally extensive and hydraulically continuous beneath the INTEC facility. Recent investigations (Forsythe, 2003) have modified this conceptual model to suggest that the perched water beneath the former percolation ponds and perched water beneath the tank farm are two distinct shallow perched water zones in part from the lack of extensive interbed continuity.

The lateral continuity of interbeds in relation to the scale of the surface infiltration, the lithology of the interbed, as well as the volume of water applied to the soil surface can result in either minor impedance to recharge or act as an effective barrier to episodic recharge. Analysis of drilling logs near the 36-ha (88-acre) SDA indicates that approximately 10% of the boreholes did not intercept either the B–C or C–D interbeds (INEEL, 2001). Although both of these interbeds are considered to be laterally continuous, at the scale of the SDA, numerous gaps in the interbeds could result in recharge bypassing these interbeds. At the smaller scale LSIT site, water moves essentially vertical downward in the basalt until it reaches the first sedimentary interbed. Although only two wells were drilled through the B–C interbed at the LSIT, neutron and natural γ log interpretations from these wells indicated a slow wetting of the interbed and support the concept that the interbed acts as a semipermeable barrier for water (Wood and Norrell, 1996). In contrast, data from the larger-scale spreading area tracer test suggest that the rapid tracer detection in the groundwater beneath the spreading areas (22 m d^{-1}) indicates that the sedimentary interbeds are not effective barriers to vertical flow at least under ponded infiltration conditions (Nimmo et al., 2002). It is likely that the interbeds beneath the spreading areas are likely not completely continuous and allowed water to bypass the interbeds (Item 10 in Fig. 5) and continue rapidly downward.

Depending on the flux of the percolating water and the lateral continuity of the interbed, a portion of the water will perch on these interbeds to produce a more steady-state infiltration condition. Perched water conditions exist on the interbeds beneath the SDA due to episodic snowmelt and from lateral spreading from the Big Lost River or the spreading areas at the deeper interbeds. Although perched water on the interbeds likely contributes to lateral spreading of contamination in the subsurface, it also impedes the rapid wetting front advance through the basalt fractures. Subsequent infiltration through the interbeds would result in a more temporally uniform infiltration event below the interbeds. Analysis of the advanced tensiometer measurements confirms that near steady-state conditions exist in portions of the deeper subsurface (McElroy and Hubbell, 2004).

Using a unit gradient approach, a number of investigators have attempted to use hydraulic analyses from soil cores collected during drilling campaigns to estimate the infiltration flux through the interbeds. Magnuson and McElroy (1993) assumed a unit gradient and used data collected from soil cores to estimate the infiltration rate at the 73-m (C–D) interbed. They estimated the rate of infiltration to be between 4 and 10 cm yr^{-1} (1.1 and 2.7×10^{-4} m d^{-1}). McElroy and Hubbell (2004) used advanced tensiometer data to 74 m to indicate large-scale unit gradient conditions in the vadose zone at the SDA. Advanced tensiometers data were used to estimate recharge through the B–C and C–D interbeds (McElroy and Hubbell, 2003). They used water potential measurements from the B–C interbed, ranging from -30 to -195 cm (-3 to -19 kPa), to estimate steady-state flux rates of 1.6 to >21 000 cm yr^{-1} (4.4×10^{-5} m d^{-1} to $>5.8 \times 10^{-1}$ m d^{-1}). In the C–D interbed, the measured water potentials were lower and ranged from -109 to -360 cm (-10 to -36 kPa) and corresponded with flux estimates from 1.4 to 32 cm yr^{-1} (3.8×10^{-5} to 8.8×10^{-4} m d^{-1}). They discarded the high B–C flux calculations as likely not meeting the assumptions of homogeneity of the interbed material or local unit gradient conditions and considered that a deep recharge rate in the range of 1 to 32 cm yr^{-1} (2.7×10^{-5} to 8.8×10^{-1} m d^{-1}) was appropriate.

SUMMARY

Results of large-scale field experiments and the analyses of long-term monitoring data at INEEL waste sites have provided insight to describe water movement in the highly heterogeneous vadose zone beneath the INEEL. This paper attempted to integrate the results for two large-scale field experiments conducted at the INEEL (Dunnivant et al., 1998; Nimmo et al., 2002) that approach the size of the waste sites with results of long-

term monitoring from two INEEL facilities (SDA and INTEC) that have extensive vadose zone monitoring networks.

The temporal and spatial distribution of water available for infiltration is unique for the SDA and INTEC. The evaluation of the recharge sources is complicated by the type and intensity of precipitation, time of the year, alterations of surficial soils, number of potential anthropogenic sources of water near the surface, and infiltration from rivers and intermittent surface water ponding during spring melt events and summer thundershowers. Infiltration inside the SDA is estimated to be approximately 30% of the natural precipitation, as compared with approximately 5% outside the SDA due to disturbance of the surficial soil and reduction in vegetation. Temporal surface ponding and past episodic flooding are thought to be the primary contributing factors to the observed migration of dissolved-phase contaminants at the SDA. The identification of water sources at INTEC has been complicated due to colocated large volume recharge sources within and near the facility.

Analysis of long-term monitoring data and the results for two large-scale field tests have resulted in a general conceptual model of water movement in the vadose zone beneath the INEEL. Once water has percolated past the root zone the presence of the surficial sediment–basalt interface produces some perching of the percolated water with limited lateral movement. Water movement in basalt formations is mostly in preferential pathways due to the complex connectivity of the fractures, is gravity dominated, and results in mostly rapid vertical flow, especially under conditions of positive hydrostatic head. Detection of the wetting front is typically not sequential with depth and has been shown to vary between episodic infiltration events. At the basalt–sediment interface, perched water is often detected and has resulted in more lateral spreading of recharge than at the surficial sediment–basalt interface. Recharge of surface water far from the facilities can influence the development and lateral movement of perched water at the sedimentary interbeds. Lateral extent and mechanisms associated with the interbed that create a lower permeability zone control the lateral extent and connectivity of perched water bodies. Gaps in the sedimentary interbeds will allow some of the recharge water to bypass the interbeds and rapidly continue toward the aquifer. However, if the interbed is mostly continuous, it will cause significant lateral spreading along topographic contours, and may allow some of the water to infiltrate through the interbed, resulting in a nearly steady-state percolation flux beneath the interbed.

A number of implications for the INEEL waste area groups can be generalized from these results. First, controlling the amount and temporal and spatial distribution of the infiltration flux at the soil surface is important. The amount and lateral extent of water perching in the vadose zone at the INEEL is correlated with the volume and distribution of water infiltration at the soil surface. If these positive hydrostatic head zones could be eliminated, the rate of water movement through the fractured basalt formation would be greatly diminished. Second, defining gaps in interbeds is necessary for assessment of fast flow pathways to the underlying aquifer. Continuity of the interbed in relation to the aerial extent of the recharge source is important in determining whether the interbeds will significantly impede vertical water movement at the basalt–sedimentary interface. Finally, the influence of nearby surface water sources should be investigated as to their influence of perched water beneath the facilities. Results from tracer studies discussed in this paper have indicated significant lateral movement of water at the deeper sedimentary interbeds and suggest a mechanism for lateral spreading of potential contaminated water beneath the facilities.

ACKNOWLEDGMENTS

This work was conducted at the Idaho National Engineering and Environmental Laboratory under DOE Idaho Operations Office Contract DE-AC07-99ID13727 BBWI and partially funded by the Environmental Systems Research and Analysis program and Ms. Gail Olson of the INEEL.

REFERENCES

Bishop, C.W. 1996. Soil moisture monitoring results at the Radioactive Waste Management Complex of the Idaho National Engineering Laboratory, FY-96, FY-95, and FY-94. INEL-96/97. Idaho National Engineering and Environmental Laboratory, Lockheed Martin Idaho Technologies Company, Idaho Falls, ID.

Cecil, L.D., T.M. Beasley, J.R. Pittman, R.L. Michel, P.W. Kubik, P. Sharma, U. Fehn, and H.E. Gove. 1992. Water infiltration rates in the unsaturated zone at the Idaho National Engineering Laboratory estimated from chlorine-36 and tritium profiles, and neutron logging. *In* Y.K. Kharaka and A.S. Meest (ed.) Proc. of the 7th International Symposium on Water-Rock Interaction—WRI-7, Park City, UT.

Cecil, L.D., B.R. Orr, T. Norton, and S.R. Anderson. 1991. Formation of perched ground-water zones and concentrations of selected chemical constituents in water, Idaho National Engineering Laboratory, Idaho, 1986–88. USGS Water-Resources Investigations Rep. 91-4166, DOE/ID-22100. Idaho National Engineering Laboratory, Idaho Falls, ID.

Clawson, K.L., G.E. Start, and N.R. Ricks. 1989. Climatography of Idaho National Engineering Laboratory, 2nd. ed. DOE/ID-12118. USDOE Idaho Operations, Idaho Falls, ID.

Dunnivant, F.M., M.E. Newman, C.W. Bishop, D. Burgess, J.R. Giles, B.D. Higgs, J.H. Hubbell, E. Neher, G.T. Norrell, M.C. Pfiefer, I. Porro, R.C. Starr, and A.H. Wylie. 1998. Water and radioactive tracer flow in a heterogeneous field-scale system. Ground Water 36:949–958.

Forsythe, H.S. 2003. Phase I monitoring well and tracer study report for Operable Unit 3-13, Group 4, perched water. DOE/ID-10967, Rev. 2. DOE-ID.

Holdren, K.J., B.H. Becker, N.L. Hampton, L.D. Koeppen, S.O. Magnuson, T.J. Meyer, G.L. Olson, and A.J. Sondrup. 2002. Ancillary basis for risk analysis for the Subsurface Disposal Area. Ext. Rep. INEEL/EXT-02-01125. Idaho National Engineering and Environmental Laboratory, Idaho Falls, ID.

Hubbell, J.M., E.D. Mattson, J.B. Sisson, and D.L. McElroy. 2002. Water potential response in fractured basalt from infiltration events. *In* M.N. Sara and L.G. Everett (ed.) Evaluation and remediation of low permeability and dual porosity environments. ASTM STP 1415. ASTM International, West Conshohocken, PA.

Hull, L.C., and C.W. Bishop. 2004. Fate of brine applied to unpaved roads at a radioactive waste subsurface disposal area. Available at www.vadosezonejournal.org. Vadose Zone J. 3:190–202 (in this issue).

INEEL. 2001. Uncertain predictions of contaminant behavior at INEEL: A roadmap for addressing current limitations through vadose zone studies. INEEL External Rep. INEEL/EXT-2001-00552, Draft Rev 0. Idaho National Engineering and Environmental Laboratory, EGG&G Idaho, Idaho Falls, ID.

Irving, J.S. 1993. Environmental resource document for the Idaho National Engineering Laboratory. EGG-WMO-10279. Idaho National Engineering and Environmental Laboratory, EGG&G Idaho, Idaho Falls, ID.

Knutson, C.F., K.A. McCormick, J.C. Crocker, M.A. Glenn, M.L. Fishel, and C.A. Whitaker. 1992. 3D RWMC vadose zone modeling. EGG-ERD-10246. USDOE Idaho Operations Office, Idaho Falls, ID.

Koslow, K.N., and D.H. VanHaaften. 1986. Flood routing analysis of a failure of Mackay Dam. EGG-EP-7-7184. Idaho National Engineering and Environmental Laboratory, EG&G Idaho, Idaho Falls, ID.

Magnuson, S.O., and D.L McElroy. 1993. Estimation of infiltration from in situ moisture contents and representative moisture characteristic curves for the 30′, 110′ and 240′ interbeds. EG&G Idaho Engineering Design File RWM-93-001. EG&G, Idaho Falls, ID.

Magnuson, S.O., and A.J. Sondrup. 1998. Development, calibration, and predictive results of a simulator for subsurface pathway fate and transport of aqueous- and gaseous-phase contaminants in the Subsurface Disposal Area at the Idaho National Engineering and Environmental Laboratory. INNEL/EXT-097-00609. Idaho National Engineering and Environmental Laboratory, Lockheed Martin Idaho Technologies Company, Idaho Falls, ID.

Martian, P. 1995. UNSAT-H infiltration model calibration at the Subsurface Disposal Area, Idaho National Engineering Laboratory. INEL-95/0596. Idaho National Engineering and Environmental Laboratory, Lockheed Martin Idaho Technologies Company, Idaho Falls, ID.

Martian, P., and S.O. Magnuson. 1994. A simulation study of infiltration into surficial sediments at the Subsurface Disposal Area. EGG-WM-11250. Idaho National Engineering Laboratory, EG&G Idaho, Idaho Falls, ID.

McElroy, D.L. 1990. Vadose zone monitoring at the Radioactive Waste Management Complex at the Idaho National Engineering Laboratory 1985–1989. EGG-WM-11066. Idaho National Engineering Laboratory, EG&G Idaho, Idaho Falls, ID.

McElroy, D.L. 1993. Soil moisture monitoring results and the Radioactive Waste Management Complex of the Idaho National Engineering Laboratory. Idaho National Engineering and Environmental Laboratory, EGG&G Idaho, Idaho Falls, ID.

McElroy, D.L., and J.M. Hubbell. 2003. Advanced tensiometer monitoring results from the deep vadose zone at the Radioactive Waste Management Complex. Ext. Rep. INEEL/EXT-02-01276. Idaho National Engineering and Environmental Laboratory, Idaho Falls, ID.

McElroy, D.L., and J.M. Hubbell. 2004. Evaluation of the conceptual flow model for a deep vadose zone system using advanced tensiometers. Vadose Zone J. 3:170–182 (in this issue).

Nimmo, J.R., K.S. Perkins, P.E. Rose, J.P. Rousseau, B.R. Orr, B.V. Twining, and S.R. Anderson. 2002. Kilometer-scale rapid transport of naphthalene sulfonate tracer in the unsaturated zone at the Idaho National Engineering and Environmental Laboratory. Vadose Zone J. 1:89–101.

Nimmo, J.R., J.P. Rousseau, K.S. Perkins, K.G. Stollenwerk, P.D. Glynn, R.C. Bartholomay, and L.L. Knobel. 2004. Hydraulic and geochemical framework of the Idaho National Engineering and Environmental Laboratory vadose zone. Vadose Zone J. 3:6–34 (in this issue).

Smith, R.P. 2004. Geologic setting of the Snake River Plain Aquifer and vadose zone. Vadose Zone J. 3:47–58 (in this issue).

Vigil, M.J. 1988. Estimate of water in pits during flooding events. Engineering Design File BWP-12, EG&G Idaho Inc., Project file 3X2MPP130. Idaho National Engineering and Environmental Laboratory, Idaho Falls, ID.

Wood, T.R., and G.T. Norrell. 1996. Integrated large-scale aquifer pumping and infiltration tests, groundwater pathways. Summary Rep. OU 7-06 INEL-96/0256. Lockheed Martin Idaho Technologies Company, Idaho Falls, ID.